Int. J. Bio-Inorg. Hybd. Nanomat., Vol. 1, No. 3 (2012), 199-207

International Journal of Bio-Inorganic Hybrid Nanomaterials

Structural, Electrical and Optical Properties of Molybdenum Oxide Thin Films Prepared by Post-annealing of Mo Thin Films

Kaykhosrow Khojier[1*], Samira Zolghadr[2], Naser Zare[2]

[1] *Department of physics, Chalous branch, Islamic Azad University, Chalous, Iran*
[2] *Department of physics, factually of science, Central Tehran branch, Islamic Azad University, Tehran, Iran*

Received: 4 July 2012; Accepted: 6 September 2012

ABSTRACT

Molybdenum thin films with 50 and 150 nm thicknesses were deposited on silicon substrates, using DC magnetron sputtering system, then post-annealed at different temperatures (200, 325, 450, 575 and 700°C) with flow oxygen at 200 sccm (standard Cubic centimeter per minute). The crystallographic structure of the films was obtained by means of x-ray diffraction (XRD) analysis. An atomic force microscope (AFM) and a scanning electron microscope (SEM) were employed to investigate the samples surface morphology. A four point probe instrument and a spectrophotometer were used for electrical resistivity and transmittance spectrum measurements, respectively. XRD results showed a MoO_3 polycrystal (single phase) for annealed samples at 450 and 575°C, while annealed sample at the highest temperature (700°C) had a mixed phase of MoO_3 and Mo_9O_{26}. Both the grain size and the surface roughness of the samples increased with annealing temperature. The electrical resistivity and transmittance spectrum of the films increased with increasing of annealing temperature up to 575°C, while an increase in annealing temperature to 700°C had an inverse effect. It was also observed that the thicker films (with 150 nm thickness) had lower resistivity and transmission.

Keyword: Thin films; Molybdenum oxide; Crystallography; Morphology; Resistivity; Transmittance spectrum.

1. INTRODUCTION

Molybdenum oxide (MoO_3) is a metal oxide characterized by an intermediate energy gap (~ 2.8 eV) that falls within the visible range. MoO_3 can exist in three crystalline polymorphs: a stable

(*) Corresponding Author - e-mail: khojier@iauc.ac.ir

orthorhombic phase (α-MoO_3), a metastable monoclinic phase (β-MoO_3), and an open hexagonal structure [1, 2].

MoO_3 thin films have their optical absorption peak close to the human eye sensitivity peak [3, 4].This property makes MoO_3 thin films very attractive for applications in optoelectronic devices [5]. These compounds show photochromic [6, 7], electrochromic [4, 8-11], and thermochromic [12] effects, which make them very important for smart windows and display applications. MoO_3 are potentially useful in the fabrication and development of electronic information displays and other optical memory devices [13-15]. MoO_3 thin films also have been found to be very sensitive to various gases such as NO, NO_2, CO, H_2 and NH_3 in the temperature range of 300-600°C [16-21].

In all these practical applications of MoO_3, the preparation method, control of growth, crystal structure, chemical composition, and electronic properties of MoO_3 thin films are of high importance. Hence, characterization of structural, electrical and optical properties of MoO_3 thin films prepared using different deposition techniques and correlation between structural and different properties of these films play an important role in their technical applications.

Different techniques, including sputtering [22-24], sol-gel [25], molecular beam epistaxis [1], chemical vapor deposition [26, 27], pulse laser deposition [28], thermal evaporation [29], e-beam deposition and post-annealing [30], and photo-chemical metal organic deposition (PMOD) [31] have been used by researchers.

In this work, we have used combination of DC sputtering for deposition of Mo thin films on Si substrates followed by annealing of Mo thin films of different thicknesses with flow of oxygen at different annealing temperature. This technique provided different conditions for investigation of crystallography phase development of the produced samples by variation of both film thickness and annealing temperature.

Different physical properties of the produced samples are also investigated and correlated with their structural characteristics.

2. EXPRRIMENTAL DETAIL

2.1. Film preparation

Molybdenum thin films of 50 and 150 nm thicknesses were deposited by means of DC magnetron sputtering system using a circular sputtering target (99.998% purity) of 76 mm diameter and 1 mm thickness. The target to substrate distance was 10 cm. A continuously variable DC power supply of 750 V and 125 mA was used as power source for sputtering. The thicknesses and deposition rate of these Mo films were checked in situ using a quartz crystal monitor (6 MHz gold, Inficon Company, USA) located near the substrate during the sputtering process. Molybdenum thin films were deposited at a deposition rate of 3 Å/s. The base pressure was $\times10^{-5}$ mbar, achieved with a diffusion pump coupled with a rotary pump that was changed to 3.2×10^{-2} mbar after presence of Argon. The purity of argon gas in this work was 99.998% and controlled by mass flow controller.

The substrates for the deposition were 20 ×20 mm^2 single crystal of Si(400) (n-type). The substrates were ultrasonically cleaned in heated acetone then etalon and were dried by argon gas flow. Post-annealing of Mo/Si films were performed by a tube furnace at five different temperatures (200 to 700°C in steps of 125°C) with flow of oxygen (purity of 99.98%) at 200 sccm. The samples were reached the selected annealing temperature with a thermal gradient of 5 degree/min and were kept at the annealing temperature 120 min, then gradually cooled down to room temperature.

2.2. Film characterization

Nanostructure and crystallographic orientation of the samples were obtained using a Philips XRD X'pert MPD Diffractometer (Cu Kα radiation) with a step size of 0.02° and count time of 1 s per step. Surface morphology and roughness of the samples were obtained using AFM (Auto probe PC, Park Scientific Instrument, USA) and SEM (Leo-440i, UK) analyses. The electrical resistivity of the samples was measured by a four point probe

instrument at room and 60°C temperatures, while transmittance spectrum of samples was obtained by a spectrophotometer (Spectrophotometer UV-VIS-NIR VARIAN Cary 500, USA).

3. RESULT AND DISCUSSION

3.1. Crystallographic structure

X-ray diffraction patterns of Mo/Si selected samples (as deposited and annealed) with 50 nm thickness are shown in Figure 1. X-ray diffraction pattern of as deposited sample depicts a peak at 40.51° that can be related to Mo(110) crystallographic orientation (with reference to JCPDS Card No.: 42-1120, 2θ=40.516°, system: cubic and space group: 229). By annealing at 200°C temperature the intensity of Mo(110) peak decreased and a very weak hump observed approximately at 25.7°. By increasing of annealing temperature to 325°C this procedure repeated, so that Molybdenum peak intensity decreased and the hump intensity amplified.

This hump can be attributed to three diffraction lines of molybdenum oxide MoO_3 phase that are (110), (040) and (021) crystallographic orientations, respectively (with reference to JCPDS Card No.: 35-0609, 2θ=23.339°, 25.699° and 27.339° system: orthorhombic and space group: 62). At annealed sample at 450°C temperature Mo(110) peak was quite omitted, and the hump was separated to three peaks MoO_3(110), MoO_3(040), MoO_3(021) at 23.37°, 25.63° and 27.35°. Furthermore, other peaks were observed in this sample. These peaks were (020), (111), (041), (060), (061), (002), (211), (112) and (132) crystallographic orientations at 12.77°, 33.77°, 35.47°, 38.95°, 46.29°, 49.29°, 52.79°, 55.21° and 58.55°, respectively. These peaks can be related to MoO_3 phase of molybdenum oxide (with reference to JCPDS Card No.: 35-0609, 2θ=12.780°, 33.759°, 35.499°, 38.979°, 46.319°, 49.259°, 52.799°, 55.199°, and 58.579° system: orthorhombic and space group: 62). By an increase in annealing temperature to 575°C any new peak wasn't observed, but the intensity of peaks were changed (approximately increased). In XRD pattern of sample which formed at annealing temperature of 700°C exist alone (110), (040) and (021) crystallographic orientations of MoO_3 phase (but with low intensity) and other peaks were omitted. In this sample a number of new diffraction lines were also obvious at 15.37°, 20.33°, 21.61°, 24.97°, 26.13°, 30.17° and 34.27° that can be attributed to Mo_9O_{26} phase of molybdenum oxide and (-202), (-203), (-401), (-211), (112), (-213) and (-214) crystallographic orientations (with reference to JCPDS Card No.: 05-0442, 2θ=15.397°, 20.305°, 21.604°, 24.992°, 26.110°, 30.157° and 34.276° system: monoclinic and space group: 13), respectively.

Similar to this variation of crystallographic structure with annealing temperature observed for Mo/Si samples with 150 nm thickness, so that the annealed samples at different thickness (50 and 150 nm) have similar crystallographic structure.

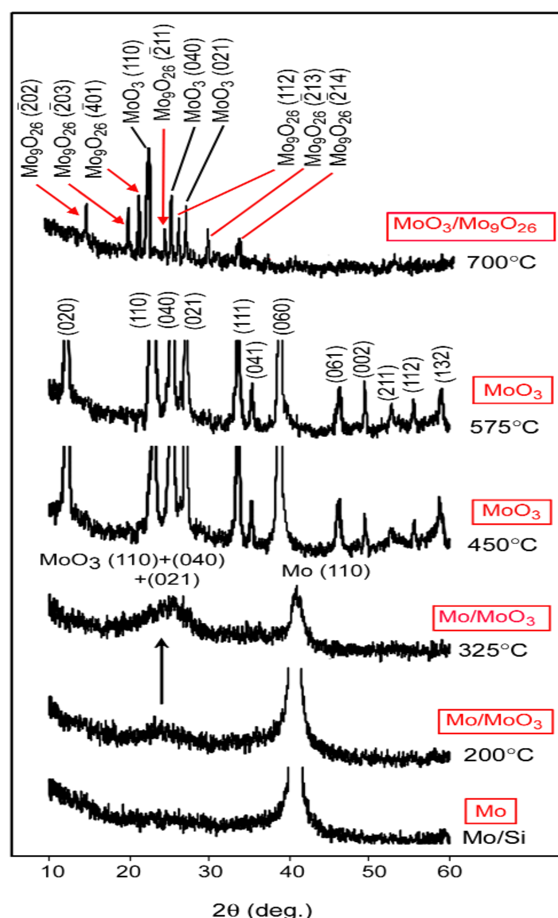

Figure 1: X-ray diffraction pattern of Mo/Si thin films (unheated and post-annealed at different annealing temperature).

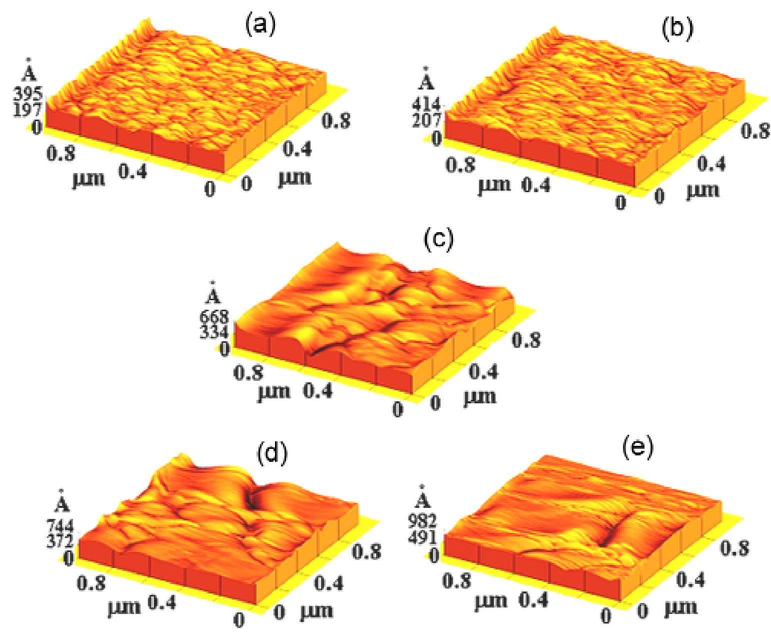

Figure 2: *3D AFM images of molybdenum oxide thin films which annealed at a) 200°C, b) 325°C, c) 450°C, d) 575°C and e) 700°C.*

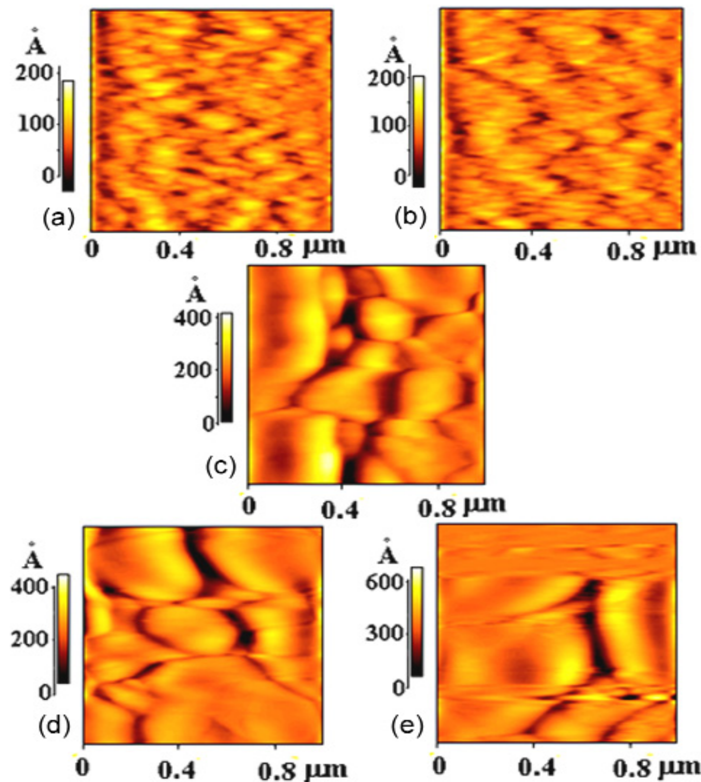

Figure 3: *2D AFM images of molybdenum oxide thin films which annealed at a) 200 °C, b) 325°C, c) 450°C, d) 575°C and e) 700°C.*

In fact, the results showed that the Mo annealed samples (independent of thickness) at 450 and 575°C were polycrystal of MoO_3. The sample which annealed at 700°C had mixed phase of MoO_3 and Mo_9O_{26} too.

3.2. Surface physical morphology

3D and 2D AFM images of molybdenum oxide selected films with 50 nm thickness are shown in Figures 2 and 3, respectively. The rms parameter of surface roughness and the size of the grains (calculated from 2D AFM images, using JMicrovision Code) of all samples are also given in Table 1.

The results show that the increment of annealing temperature caused the increment of grain size and surface roughness, while the thicker films have larger value of grain size and surface roughness. This is due to increased surface diffusion (mobility) which causes the coalescence of the grains which in turn produces larger and deeper valleys between these newly formed grains, hence higher surface roughness is obtained.

Figure 4, depicts SEM images of selected samples with 50 nm thickness (as deposited and annealed Mo/Si thin films). The SEM images are consistent with AFM images, so that the sizes of the grains increase by increasing of annealing temperature.

3.3. Electrical properties

Results of DC resistivity measurement obtained using a four point probe instrument (at room and 60°C temperatures) is discussed in this section. In order to investigate the influence of possible (low frequency) charging effects at the electrical contacts and leads, current-voltage (I-V) curves were recorded, scanning the voltage both in increasing and decreasing increments. Figure 5, depicts the results for selected sample with 50 nm thickness and post-annealed at 200°C. The results measurements in both of the increasing and decreasing direction of the voltage are shown in this Figure. However, it should be noted that the current was kept low enough, in order to not heat up the samples.

Linear I-V curves were obtained for all samples, independent of the scan direction, and there was no indication of hysteresis effect. In order to investigate the anisotropy effect in these samples, the I-V curves measurements were also carried out in four different directions on the samples, namely, two vertical (along the sample length and normal to the length) and two diagonal directions. The values of average resistivity for all samples are given in Table 1 and Figure 6. The results show that the resistivity increases by increasing of annealing

Table 1: *Information of samples and results of AFM, four point probe and spectrophotometry analyses (* AoT: Average of Transmittance).*

Sample No.	Thickness (nm) ± 2	T_a (°C) ± 5	Grain diameter (μm) ± 0.02	rms (Å)	Resistivity (μΩ.cm) RT	Resistivity (μΩ.cm) 60 °C	AoT* (%)
Z-1	50	200	0.07	23.7	1370	1130	5
Z-2	50	325	0.11	24.5	3810	3400	22
Z-3	50	450	0.18	58.2	5401	5000	58
Z-4	50	575	0.25	62.5	6940	6380	71
Z-5	50	700	0.34	65.7	5310	4660	57
Z-6	150	200	0.09	25.1	860	770	2
Z-7	150	325	0.14	25.7	2940	2580	11
Z-8	150	450	0.19	63.3	4640	4200	41
Z-9	150	575	0.28	68.6	5860	5100	54
Z-10	150	700	0.37	69.8	4140	3620	41

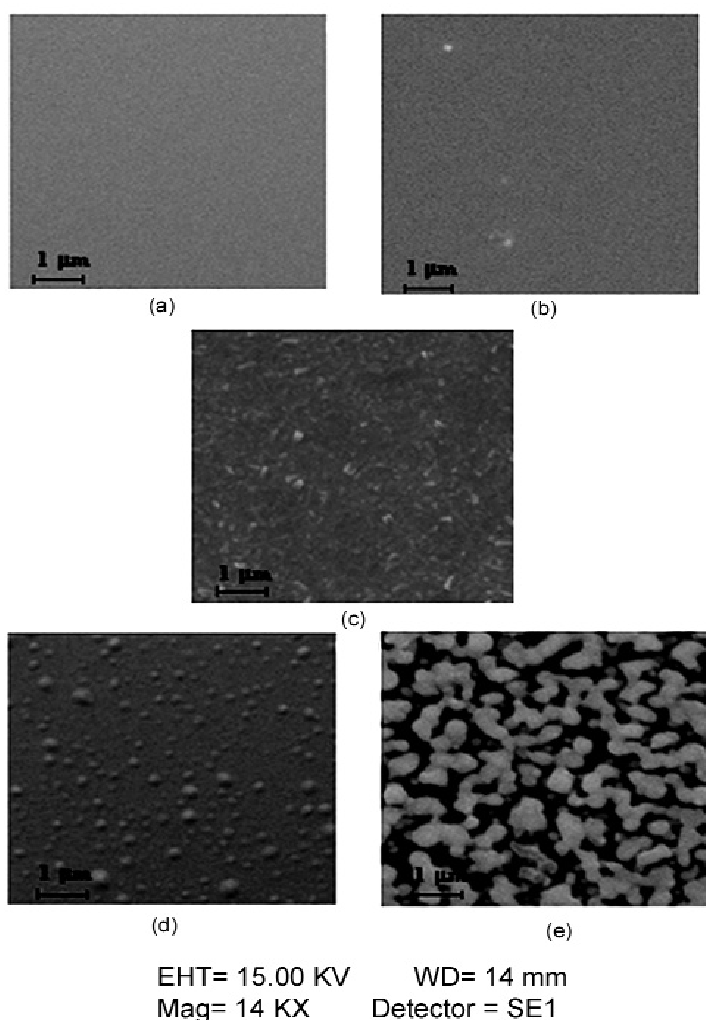

Figure 4: *SEM images of molybdenum oxide thin films which annealed at a) 200°C, b) 325°C, c) 450 °C, d) 575°C and e) 700°C.*

temperature up to 575°C and then decreases. A similar kind of resistivity behavior as a function of annealing temperature (in the range of 200-500°C temperatures) for the films which produced by e-beam and post-annealed for 10 min had been reported earlier by Lin and et al. [30]. The results also showed that the thicker films had lower resistivity. These behaviours can be explained as follow:

It should be noted that the number of oxygen vacancies in the films increase by increasing of annealing temperature up to 575°C that caused the increase of film resistivity. Furthermore, in formed samples at low annealing temperature the oxygen atoms bonding with the molybdenum atoms are not enough (due to the low influence of oxygen atoms) and the remainder amorphous molybdenum atoms act as donors and can provide free electrons. With these free electrons, the films have a high carrier density and low resistivity. But at formed samples at higher annealing temperature due to the more influence of oxygen atoms, there are sufficient oxygen atoms integrated with the molybdenum atoms that caused only a few free electrons.

Decreasing of resistivity of films which annealed at 700°C can be also related to escaping of oxygen atoms from MoO_3 lattice at the highest annealing temperature that caused decreasing of

oxygen vacancies in the films(as can be seen in XRD pattern).

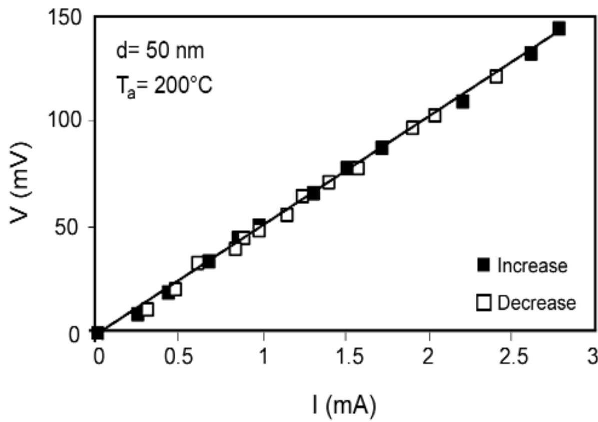

Figure 5: *Variation of voltage as a function of current of selected sample (sample # Z-1) at room temperature.*

Scattering of carriers from the film surface is effective in conductivity when the film thickness is comparable with mean free path of carriers. For this reason, increasing of thickness decreased scattering of carriers from film surface and caused decreasing of resistivity molybdenum oxide thin films with 150 nm thickness.

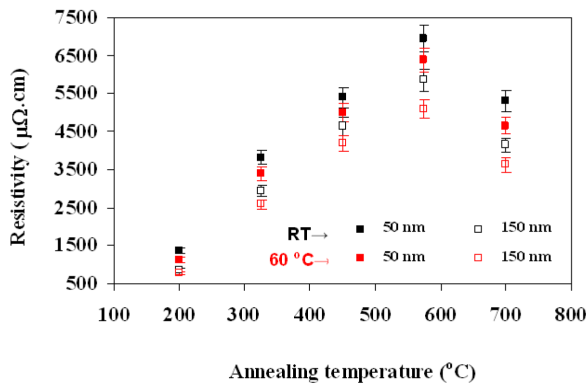

Figure 6: *variation of resistivity of molybdenum oxide thin films prepared at this work as a function of annealing temperature.*

The electrical results also showed that increasing of environment temperature caused decreasing of film resistivity, so that the resistivity which measured at 60°C temperature was lower than measured resistivity at room temperature. This decrease is related to production of free carriers due to the obtained energy from the increasing of environment temperature.

3.4. Optical investigations

Transmittance spectra in the range of 900-1800 nm (for selected samples, with 50 nm thickness) at different annealing temperature are shown in Figure 7, when average of transmittance spectrum of all samples is given in Table 1. It should be noted that restriction in wavelength of transmittance spectra is due to nature of silicon substrate.

The results show that transmittance spectrum of samples increase by increasing of annealing temperature up to 575°C that can be attributed to increasing of number of oxygen vacancies in the films. This increase of transmittance spectra can indicate to increasing of optical band gap by increasing of annealing temperature up to 575°C and is consistent with Lin results for MoO_3 thin films [30]. But transmittance spectra decrease (or perhaps band gap decrease) by an increase in annealing temperature to 700°C. This behavior can be related to the change of crystallographic structure from orthorhombic structure of MoO_3 phase to monoclinic structure of Mo_9O_{26} phase, and escaping of oxygen atoms from MoO_3 lattice at the highest annealing temperature (consistent with XRD pattern).

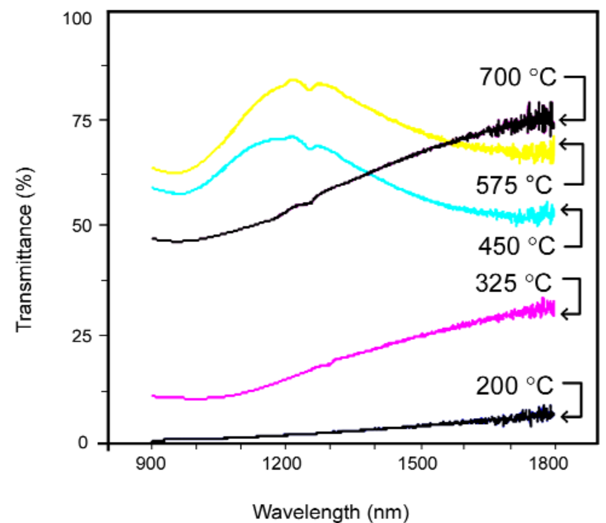

Figure 7: *Transmittance spectra (in the range of 900-1800 nm) of molybdenum oxide thin films with 50 nm thickness at different annealing temperatures.*

4. CONCLUSIONS

Molybdenum Oxide thin films prepared by post-annealing of Mo/Si(400) thin films (with 50 and 150 nm thickness) at different annealing temperature (200-700°C) were studied.

Nanostructure and surface morphology of these layers were considered by XRD, AFM and SEM, when a four point probe instrument was employed for resistivity measurements. The result showed: a) the annealed films at 450 and 575°C were a ploycrystal of MoO_3 with orthorhombic structure. b) The sample which annealed at 700°C had combined phase of MoO_3 and Mo_9O_{26}. c) The variation of crystallographic structure of samples as a function of annealing temperature was independent of films thickness. d) The size of the grains and surface roughness increased by increasing of annealing temperature. e) The resistivity increased by increasing of annealing temperature up to 575°C and then decreased. f) The thicker samples had lower resistivity. g) Increasing of environment temperature caused decreasing of resistivity. h) The transmittance spectra of films increased by increasing of annealing temperature up to 575°C, and then decreased.

ACKNOWLEDGMENTS

This work was carried out by the support of the Islamic Azad University, Chalous branch and central Tehran branch. The authors are also grateful to Dr. Safari Sabet.

REFERENCES

1. Altman E.I., Droubay T., Chambers S.A., *Thin Solid Films*, **414**(2002), 205-215.
2. Ivanova T., Gesheva K., Szekeres A., J. *Solid State Electrochem*, **7**(2002), 21-24.
3. Brenede J.C., Alaoui Z.K., Manai N., *Thin Solid Films*, **235**(1993), 25-29.
4. Gesheva K., Szekeres A., Ivanova T., *Sol. Ene. Mat. Sol. Cells*., **76**(2003), 563-576.
5. Zhou J., Xu N.S., Deng S.Z., Chen J., She J.C., Wang Z.L., *Adv. Mater*., **15**(21) (2003), 1835-1840.
6. Yao J.N., Hascimoto K., Fujishima A., *Nature*, **355**(1992), 624-626.
7. Tokarz-Sobieraj R., Hermann K., Witko M., Blume A., Mestl G., Schlogl R., *Surface Science*, **489**(2001), 107-125.
8. Guerfi A., Dao L.H., J. *Electrochem. Soc.*, **136**(1989), 2435-2436.
9. Hamelmann F., Gesheva K., Ivanova T., Szekeres A., Abrashev M., Heinzmann U., *J. Optoelectron. Adv. Mater.*, **7(**1) (2005), 393-396.
10. Miyata N., Akiyoshi S., *J. Appl. Phys.* **58**(4) (1985), 1651-1655.
11. Gesheva K., Ivanova T., Popkirov G., Hamelmann F., *J. Opt. Elect. Adv. Mater*, **7**(1) (2005), 169-175.
12. Chudnovskii F.A., Schaefer D.M., Gavrilyuk A.I., Reifenberger R., *Appl. Sur. Sci.*, **62**(1992), 145-149.
13. C.G. Granqvist, 1995. *Handbook of Inorganic Electrochromic Materials*, Elsevier, Amsterdam,
14. McEvoy T.M., Stevenson K.J., *J. Am. Chem. Soc.*, **125**(2003), 8438-8439.
15. Husssain Z., *J. Electron. Mat*., **31**(2002), 615-630.
16. Di Giulio M., Manno D., Micocci G., Serra A., Tepore A., *Phys. Status Solidi A*., **168**(1998), 249-256.
17. Ferroni M., Guidi V., Martinelli G., Sacerdoti M., Nelli P., Sberveglieri G., *Sensors Actuators B*, **48**(1998), 285-288.
18. Imawan C., Steffes H., Solzbacher F., Obermeier E., *Sensors Actuators B.*, **77**(2001), 346-351.
19. Mutschall D., Holzner K., Obermeier E., *Sensors Actuator*, **36**(1996), 320-324.
20. Comini E., Yubao L., Brando Y., Sberveglieria G., Chem. Phys. Lett., **4**(2005), 368-371.
21. Ferroni M., Guidi V., Martinelli G., Sacerdoti M., Nelli P., Sberveglieri G., *Sensor Actuator*, **48**(1998), 285-288.
22. Mohamed S.H., Kappertz O., Ngaruiya J.M., Leervad Pedersen T.P., Drese R., Wuttig M., *Thin Solid Films*, **429**(2003), 135-143.

23. Comini E., Faglia G., Sberveglieri G., Cantalini C., Passacantando M., Santucci S., Li Y., Qu W., *Sens. Actuators B Chem*., **68**(2000), 168-174.
24. Ramana C.V., Atuchin V.V., Pokrovsky L.D., Becker U., Julien C.M., *J. Vac. Sci. Technol. A.* **25**(2007), 1166-1171.
25. Hsu C.S., Chan C.C., Huang H.T., Peng C.H., Hsu W.C., *Thin Solid Films*, **516**(2008), 4839-4844.
26. Ivanova T., Gesheva K., Szekeres A., *J. Solid State Electrochem.*, **7**(2002), 17-20.
27. Martinez Guerrero R., Vargas Garcia J.R., Santes V., Gomez E., *J. Alloys Compd.*, **434** (2007), 701-703.
28. Ramana C.V., Julien C.M., *Chem. Phys. Lett.*, **428**(2006), 114-118.
29. Sian T.S., Reddy G.B., *Sol. Energy Mater. Sol. Cells.*, **82**(2004), 375-386.
30. Lin S.Y., Chen Y.C., Wang C.M., Hsieh P.T., Shih S.C., *Appl. Surf. Sci.*, **255(**2009), 3868-3874.
31. Buono-Core G.E., Cabello G., Klahn A.H., Lucero A., Nunez M.V., Torrejoa B., Castillo C., *Polyhedron*, **29**(2010), 1551-1554.